# Mesoporous Aminopropyl-Functionalized Hybrid Thin Films with Modulable Surface and Environment-Responsive Behavior

A. Calvo,[†] P. C. Angelomé,[†] V. M. Sánchez,[‡] D. A. Scherlis,[‡,§] F. J. Williams,[§,||,⊥] and G. J. A. A. Soler-Illia*[,†,‡,§,⊥]

*Gerencia de Química, CNEA, Centro Atómico Constituyentes, Av. Gral Paz 1499, San Martín B1650KNA, Buenos Aires, Argentina, DQIAyQF, FCEN, Universidad de Buenos Aires, Ciudad Universitaria, Pabellón II, C1428EHA Buenos Aires, Argentina, CONICET, Av. Rivadavia 1917, C1033AAJ Buenos Aires, Argentina, Departamento de Química de Superficies y Recubrimientos, TENARIS, Simini 250, B2804MHA Campana, Buenos Aires, Argentina., and Centro Interdisciplinario de Nanociencia y Nanotecnología, Av. Rivadavia 1917, C1033AAJ Buenos Aires, Argentina*

*Received February 29, 2008. Revised Manuscript Received May 7, 2008*

A first study of the behavior of amino functions in mesoporous hybrid thin films $M_{1-x}(Si(CH_2)_3NH_2)_xO_{2-x/2}$ ($M = Si$, Ti, Zr; $0.05 \leq x \leq 0.2$) with accessible $Im\bar{3}m$- or $Fm\bar{3}m$-derived pore mesostructures is presented. An XPS study of surface nitrogen species shows two different sites corresponding to amino and ammonium groups. The ratio of these species changes with pH and is related to the nature of M, suggesting that the interaction between the organic functions and the surface M−OH groups can be tailored to tune the surface acid−base behavior. Density functional theory (DFT) calculations were used to rationalize the XPS observations showing that $-NH_3^+$ functions irreversibly transfer a proton to neighboring $M-O^-$ surface groups. The acid−base surface properties can be further modified by adding a phosphonate "capping" on the M surface sites. Our findings have a series of interesting implications in surface functionalization: attachment of biomolecules to surfaces, design of perm-selective or philicity-selective membranes, or design of catalysts that show a well-defined organic reactive function near surface hydroxyl groups.

## Introduction

The field of mesoporous materials is nowadays expanding. The possibility of generating tuned pore arrays with controlled size and interconnection permits the design of complex cavity systems, which are promising as selective membranes or nanoreactors.[1] Mesoporous hybrid thin films (MHTFs) present a great interest for their potential in domains such as optics, electronics, chemical sensing, catalysis, separation, and so forth.[2–4] These materials are synthesized by an evaporation-induced self-assembly (EISA) process, which combines sol−gel chemistry and self-assembly of an organic surfactant template.[5] The introduction of organic or metallo-organic functions on the surface of mesopores is a step forward toward the creation of complex chemical systems with tuned reactivity.[6–8] The possibility of accommodating molecular functions with a well-defined location in space opens the path for new concepts in catalysis, separation, nanobiomaterials, and so forth.[9–14] To design complex molecular systems, a sound knowledge of the availability of the organic functions and their interactions with the pore surface is needed.

These organic functions are added either by co-condensation of a functional inorganic precursor with another precursor in the presence of templates ("one-pot" method) or by postsynthesis treatment of a mesostructured or mesoporous material, either by solution impregnation or by exposure to volatile vapors (postgrafting).[2] An advantage of "one pot"

[†] Centro Atómico Constituyentes.
[‡] Universidad de Buenos Aires.
[§] CONICET.
[||] TENARIS.
[⊥] Centro Interdisciplinario de Nanociencia y Nanotecnología.

(1) (a) Soler-Illia, G. J. A. A.; Sanchez, C.; Lebeau, B.; Patarin, J. *Chem. Rev.* **2002**, *102*, 4093. (b) Soler-Illia, G. J. A. A.; Crepaldi, E. L.; Grosso, D.; Sanchez, C. *Curr. Opin. Colloid Interface Sci.* **2003**, *8*, 109.
(2) (a) Shi, J. L.; Hua, Z. L.; Zhang, L. X. *J. Mater. Chem.* **2004**, *14*, 795. (b) Nicole, L.; Boissière, C.; Grosso, D.; Quach, A.; Sanchez, C. *J. Mater. Chem.* **2005**, *15*, 3598. (c) Soler-Illia, G. J. A. A.; Innocenzi, P. *Chem. Eur. J.* **2006**, *12*, 4478.
(3) (a) Otal, E. H.; Angelomé, P. C.; Bilmes, S. A.; Soler-Illia, G. J. A. A. *Adv. Mater.* **2006**, *18*, 934. (b) Etienne, M.; Quach, A.; Grosso, D.; Nicole, L.; Sanchez, C.; Walcarius, A. *Chem. Mater.* **2007**, *19*, 844.
(4) Sanchez, C.; Boissière, C.; Grosso, D.; Laberty, C.; Nicole, L. *Chem. Mater.* **2008**, *20*, 682.
(5) Grosso, D.; Cagnol, F.; Soler-Illia, G. J. A. A.; Crepaldi, E. L.; Amenitsch, H.; Brunet-Bruneau, A.; Bourgeois, A.; Sanchez, C. *Adv. Funct. Mater.* **2004**, *14* (4), 309.
(6) (a) Burkett, S. L.; Sims, S. D.; Mann, S. *Chem. Commun.* **1996**, 1367. (b) Macquarrie, D. J. *Chem. Commun.* **1996**, 1961. (c) Fowler, C. E.; Burkett, S. L.; Mann, S. *Chem. Commun.* **1997**, 1769.
(7) (a) Lim, M. H.; Blanford, C. F.; Stein, A. *J. Am. Chem. Soc.* **1997**, *119*, 4090. (b) Fowler, C. E.; Lebeau, B.; Mann, S. *Chem. Commun.* **1998**, 1825. (c) Hall, S. R.; Fowler, C. E.; Lebeau, B.; Mann, S. *Chem. Commun.* **1999**, 201.
(8) (a) Hoffmann, F.; Cornelius, M.; Morell, J.; Fröba, M. *Angew. Chem., Int. Ed.* **2006**, *45*, 3216. (b) Sayari, A.; Hamoudi, S. *Chem. Mater.* **2001**, *13*, 3151. (c) Stein, A.; Melde, B. J.; Schroden, R. C. *Adv. Mater.* **2000**, *12*, 1403.
(9) Anwander, R. *Chem. Mater.* **2001**, *13*, 4419.
(10) Angelos, S.; Johansson, E.; Stoddart, J. F.; Zink, J. I. *Adv. Funct. Mater.* **2007**, *17*, 2261.
(11) Liu, J.; Shin, Y.; Nie, Z.; Chang, J. H.; Wang, L.-Q.; Fryxell, G. E.; Samuels, W. D.; Exarhos, G. J. *J. Phys. Chem. A* **2000**, *104*, 8328.
(12) Dufaud, V.; Davis, M. E. *J. Am. Chem. Soc.* **2003**, *125*, 9403.
(13) Notestein, A.; Katz, J. M. *Chem. Eur. J.* **2006**, *12*, 3954.
(14) Goettmann, F.; Grosso, D.; Mercier, F.; Mathey, F.; Sanchez, C. *Chem. Commun.* **2004**, 1240.

10.1021/cm800597k CCC: $40.75 
Published on Web 06/20/2008

methods is the high control and homogeneity of the function incorporation, avoiding the problems of pore blockage associated to postgrafting with organosilanes.[2] Several organic functions have been introduced in both silica[15] or nonsilica[16] matrices. In particular, amino groups are interesting because of the possibility of creating pH-responsive charged surfaces with perm-selective properties,[17,18] biomolecule binding,[19] or creation of enzyme-like surface sites for advanced catalysis.[13,14]

The actual chemical speciation and conformation of the included organic functions are central features, because they control the reactivity and therefore the possibility of building complex chemical systems in highly controlled cavities. Relevant data have been obtained in modified mesoporous powders by X-ray photoelectron spectroscopy (XPS) or magic-angle spinning nuclear magnetic resonance (MAS NMR).[20,21] The acid−base behavior of surface amino functions found in self-assembled monolayers (SAMs)[22] and aminopropylsilane-derived thin films[23–28] has been studied by spectroscopic or titration methods. However, there is a lack of information regarding the acid−base behavior of nitrogen-modified MHTF, where the issues of function speciation, conformation, and availability are central to understanding the chemical reactivity in mesopores.[15a] This is a crucial issue for the future applications of these materials in several fields, such as sensing and protein immobilization.

In this paper the effect of amine functionalization in MHTFs and their environment response is described in detail. MHTFs with amino/ammonium functions are produced; the organic groups are located near M−OH/M−O$^-$ surface groups, for different M such as Si, Ti, and Zr. XPS shows that the ratio of ammonium/amino groups, R = [−$NH_3^+$]/[−$NH_2$], decreases when the external pH is increased depending on the nature of M. Density functional theory (DFT) calculations show that −$NH_3^+$ functions irreversibly transfer a proton to neighboring M−O$^-$ surface groups via the formation of an intermediate ionic pair that involves bending of the propylammonium function toward the −M−O$^-$ groups, leading to H-bonded surface M−OH and −$NH_2$ functional groups. The results of these calculations are used to rationalize the variation of the *R* ratio with pH and with the nature of M observed by XPS. Furthermore, adding a phosphonate "capping" on the M surface sites blocks surface −M−OH groups and increases the ammonium/amino ratio as predicted by our model.

## Experimental Methods

F127-templated $M_{1-x}(Si(CH_2)_3NH_2)_xO_{2-x/2}$ ($0 \le x \le 0.3$) with M = Si, Ti, or Zr mesoporous thin films were synthesized by a one-pot method. Precursor solutions were prepared using tetraethoxysilane (TEOS), $TiCl_4$, and $ZrCl_4$ as inorganic precursors. APTES ($(CH_3CH_2O)_3Si(CH_2)_3NH_2$) was used to introduce the amino function. Pluronics F127, $(EO)_{106}(PO)_{70}(EO)_{106}$ (EO and PO are ethylene oxide and propylene oxide monomers), was used as template. Solutions containing M:APTES:$H_2O$:EtOH:F127 with $1 - x$:$x$:10:40:0.005 composition (M = Si, Ti, Zr) were prepared. In the case of M = Si, extra acid has to be added, to protonate the amino groups and trigger hydrolysis: 0.28 mol of HCl was added for every mole of TEOS + APTES. Samples with $x = 0.2$ presented in this study are labeled S82, T82, or Z82 to denote a hybrid material $M_{0.8}(Si(CH_2)_3NH_2)_{0.2}O_{0.9}$ with M = Si, Ti, or Zr, respectively. Solutions prepared under these conditions were transparent and stable for at least 48 h at ambient temperature and can be reused several times if conserved in a freezer at −20 °C and gently restored at room temperature prior to dip-coating.

The precursor solutions were used to produce mesoporous films by dip-coating on silicon wafers under 30−50% relative humidity at 298 K (1−2 mm $s^{-1}$ withdrawing speed). Freshly deposited films were submitted to 50% relative humidity (RH) chambers for 24 h, a stabilizing thermal treatment of two successive 24 h steps at 60 and 130 °C, and a final 2 h step at 200 °C. Template was eliminated by extraction in 0.01 mol $dm^{-3}$ HCl in ethanol for three days, under stirring at 298 K. The mesostructure was conserved after the extraction process, as checked by small angle X-ray scattering (SAXS) and transmission electron microscopy (TEM); see below.

Film mesostructure was characterized by two-dimensional (2D)-SAXS at the D11A-SAXS2 line at the Laboratório Nacional de Luz Síncrotron, Campinas, SP, Brazil (LNLS), using $\lambda = 1.608$ Å, a sample−detector distance of 650 mm, and a CCD detector (3° or 90° incidence); X-ray reflectometry (XRR) measurements were performed at D10A-XRD2 line at LNLS, using $\lambda = 1.5498$ Å. Film densities were calculated from the critical angle in grazing incidence X-ray reflectivity (specular reflection).[29] A nonmesoporous sample produced following the same synthesis path but in the absence of template was used as the wall density reference for the matrix ($\rho_m$). A two-phase system was considered: the matrix ($V_m$ with dense walls, $\rho_m$), and void pores ($V_p$, with $\rho_p = 0$). The porous fraction was calculated as $f = V_p/(V_p + V_m)$. TEM measurements were made using a Philips EM-301 TEM microscope using an acceleration voltage of 60 kV.

To detect the speciation of amino/ammonium dangling groups, samples were submitted to different pH conditions, followed by Fourier transform infrared (FTIR) spectroscopy and XPS analysis. Samples were immersed in solutions at pH between 0 and 12. The pH value of the solutions was adjusted by titration of sodium hydroxide (0.2 mol $dm^{-3}$) with an adequate quantity of $HClO_4$. In solutions of moderate pH (2−9), NaOH was first titrated up to pH = 7, and the final pH was attained by subsequent addition of small quantities of $HClO_4$ or NaOH concentrated solution. As a conse-

(15) (a) Liu, N.; Assink, R. A.; Smarsly, B.; Brinker, C. J. *Chem. Commun.* **2003**, 1146. (b) Liu, N.; Assink, R. A.; Smarsly, B.; Brinker, C. J. *Chem. Commun.* **2003**, 370. (c) Cagnol, F.; Grosso, D.; Sanchez, C. *Chem. Commun.* **2004**, 1742.
(16) (a) Soler-Illia, G. J. A. A.; Angelomé, P. C.; Bozzano, P. B. *Chem. Commun.* **2004**, 2854. (b) Angelomé, P. C.; Soler-Illia, G. J. A. A. *J. Mater. Chem.* **2005**, *15*, 3903.
(17) Newton, M. R.; Bohaty, A. K.; White, H. S.; Zharov, I. *J. Am. Chem. Soc.* **2005**, *127*, 7268.
(18) Fattakhova-Rohlfing, D.; Wark, M.; Rathouský, J. *Chem. Mater.* **2007**, *19*, 2640.
(19) Yiu, H. H. P.; Wright, P. A. *J. Mater. Chem.* **2005**, *15*, 3690.
(20) Lim, M. H.; Stein, A. *Chem. Mater.* **1999**, *11*, 3285.
(21) Goletto, V.; Bled, A.-C.; Trimmel, G.; Wong Chi Man, M.; Woo, H. G.; Durand, D.; Babonneau, F. *Mater. Res. Soc. Symp. Proc.* **2002**, *726* (Q6), 14.
(22) Shyue, J. J.; De Guire, M. R.; Nakanishi, T.; Masuda, Y.; Koumoto, K.; Sukenik, C. N. *Langmuir* **2004**, *20*, 8693.
(23) Bagwe, R. P.; Hilliard, L. R.; Tan, W. *Langmuir* **2006**, *22*, 4357.
(24) George, I.; Viel, P.; Bureau, C.; Suski, J.; Lecayon, G. *Surf. Interface Anal.* **1996**, *24*, 774.
(25) Zhmud, B. V.; Pechenyi, A. B. *J. Colloid Interface Sci.* **1995**, *173*, 71.
(26) Zhmud, B. V.; Sonnefeld, J. *J. Non-Cryst. Solids* **1996**, *195*, 16.
(27) Kranias, S.; Bureau, C.; Chong, D. P.; Brenner, V.; George, I.; Viel, P.; Lecayon, G. *J. Phys. Chem. B* **1997**, *101*, 10254.
(28) Caravajal, G. S.; Leyden, D. E.; Quinting, G. R.; Maciel, G. E. *Anal. Chem.* **1988**, *60*, 1776.
(29) van der Lee, A. *Solid State Sci.* **2002**, *2*, 257.

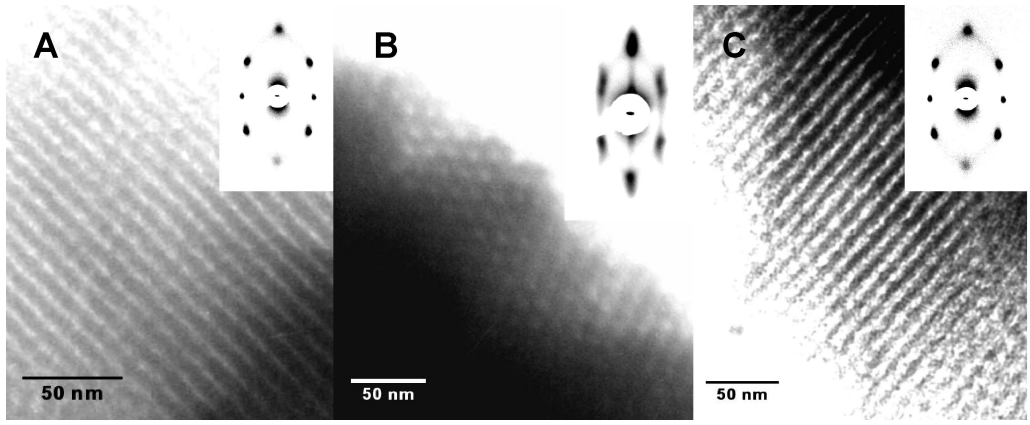


**Figure 1.** TEM pictures and SAXS data of representative MHTF samples, stabilized at 200 °C, and submitted to template extraction: (a) S82; (b) Z82; and (c) T82.

quence, the ionic force was maintained constant at 0.2 mol $dm^{-3}$ in all experiments. Each film was immersed for 20 min at ambient temperature at a given pH and subsequently rinsed several times with absolute ethanol. No pH change was observed in the solutions after film removal. The chosen immersion time was selected to appreciate changes due to pH (which occurs within 10 min of immersion) while minimizing silica dissolution, which was observed at pH > 9, and after 40 min immersion. Films submitted to a given pH and subsequent rinsing were left to dry in open flasks at ambient temperature before measuring. The addition of a second function, phenylphosphonate (PP), to Z82 and T82 was carried out immersing the films in tetrahydrofuran (THF) solutions of 0.01 mol $dm^{-3}$ of phenylphosphonic acid ($C_6H_5PO_3H_2$) at different pH values, following a protocol similar to the one described above and reference 16.

FTIR spectroscopy and diffuse reflectance infrared Fourier transform spectroscopy (DRIFTS) measurements were performed with a Nicolet Magna 560 instrument, equipped with a liquid nitrogen cooled MCT-A detector. Samples for transmission FTIR were either ground and embedded in KBr pellets or deposited on KBr thin chips used as substrate. DRIFTS measurements were performed by depositing scratched film samples on a KBr filled DRIFTS sample holder.

XPS measurements were performed using a commercial XPS system (Specs SAGE 150) equipped with a dual anode Mg/Al X-ray source and a hemispherical electron energy analyzer. Spectra were acquired using an unmonochromatic Mg Kα (1253.6 eV) source operated at 12.5 kV and 14 mA. Quoted binding energies (BEs) are referenced to the adventitious C 1s emission at 285 eV. Measurements were also conducted on powdered samples made by scratching a thin film using a conducting double stick carbon tape. Atomic ratios were calculated from the integrated intensities of core levels after instrumental and photoionization cross-section corrections. In all samples, the N:Si:M ratios evaluated by XPS reflected the global initial composition. Repeated measurements were performed along the samples, confirming reproducible XPS line positions and intensity profiles with up to 2% accuracy.

DFT calculations were carried out using the Car−Parrinello parallel code[30] included in the Quantum-ESPRESSO package,[31] which is based on DFT, periodic-boundary conditions, plane-wave basis sets, and pseudopotentials to represent the ion-electron interactions. The Kohn−Sham orbitals and charge density were expanded in plane waves up to a kinetic energy cutoff of 25 and 200 Ry, respectively. The Perdew−Burke−Ernzerhof (PBE) approach to the exchange-correlation energy[32] and Vanderbilt ultrasoft pseudopotentials[33] were adopted to compute total energies and forces. In our simulations the Ti and Si oxide surfaces were modeled using, respectively, anatase and cristobalite slabs four layers deep.

**Table 1. Structural Parameters of Mesoporous Thin Films with 20% Amino Functionalization after Stabilization at 200 °C and Template Extraction**

| system | structure | density, g $cm^{-3}$ | porosity, % | $a_{cubic}$, nm |
|---|---|---|---|---|
| S82 | $Im\bar{3}m$ | 1.55 | 24.9 | 17.8 |
| T82 | $Im\bar{3}m$ | 1.65 | 40.3 | 18.2 |
| Z82 | $Fm\bar{3}m$ | 2.32 | 24.5 | 16.7 |

## Results and Discussion

**Structural and Functional Characterization.** Figure 1 shows typical TEM and 2D-SAXS (inset) patterns corresponding to highly organized regular pore arrays with cubic-derived mesostructures ([100] oriented $Im\bar{3}m$ or [111] oriented $Fm\bar{3}m$), uniaxially distorted in the $z$ direction upon thermal treatment. Contractions are typically of 40−50%; that is, the pore height is between 6−8 nm.[34] TEM images show that the inorganic framework is continuous and does not present dark regions corresponding to Ti- or Zr-rich segregation[35] under the conditions studied; this observation is also confirmed by energy-dispersive spectrometry analysis. For the $Im\bar{3}m$ materials, typical "ladder-like" patterns are observed along the samples, corresponding to top-views of a [110] oriented mesoporous film. Micrographs corresponding to the $Fm\bar{3}m$ thin films show hexagonal-like pore arrays, corresponding to top-views of a [111] oriented mesoporous film. Typical mesostructure cell parameters obtained from SAXS patterns, film density, and porosity (evaluated by XRR[29]) are presented in Table 1. These structural results show that aminopropyl functionalized M82 (M = Si, Ti, and Zr) thin films present highly ordered mesopores with a monodispersed size distribution.

(30) Giannozzi, P.; De Angelis, F.; Car, R. *J. Chem. Phys.* **2004**, *120*, 5903.
(31) Baroni, S.; Dal Corso, A.; de Gironcoli, S.; Giannozzi, P.; Cavazzoni, P.; Ballabio, G.; Scandolo, S. Chiarotti, G.; Focher, P.; Pasquarello, A.; Laasonen, K.; Trave, A.; Car, R.; Marzari, N.; Kokalj, A. http://www.quantum-espresso.org/ (accessed November 2007).
(32) Perdew, J. P.; Burke, K.; Ernzerhof, M. *Phys. Rev. Lett.* **1996**, *77*, 3865.
(33) Vanderbilt, D. *Phys. Rev. B* **1990**, *41*, 7892.
(34) Tate, M. P.; Urade, V. N.; Kowalski, J. D.; Wei, T.-C.; Hamilton, B. D.; Eggiman, B. W.; Hillhouse, H. W. *J. Phys. Chem. B* **2006**, *110*, 9882.
(35) Soler-Illia, G. J. A. A.; Crepaldi, E. L.; Grosso, D.; Sanchez, C. *J. Mater. Chem.* **2004**, *14*, 1879.

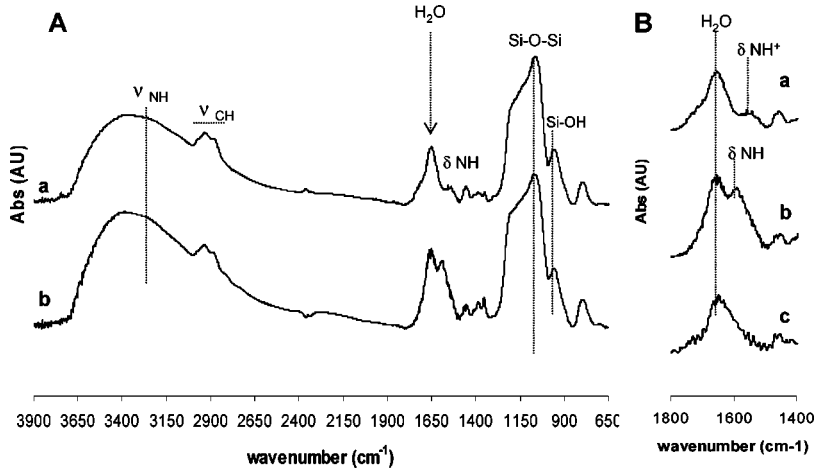


**Figure 2.** (A) DRIFTS spectra of hybrid S82 films after extraction, submitted to pH = 0 (a) and pH = 10 (b). (B) Detail of the 1400−1800 cm$^{-1}$ region, showing the bending O−H and N−H peaks for samples shown in A; an extracted F127-templated pure silica film is shown in c, for the sake of comparison. Relevant frequency regions are indicated. Curves are shifted in absorbance to facilitate visualization.

FTIR and DRIFTS spectra show the characteristic bands of the inorganic frameworks and the organic functions incorporated into the mesoporous samples. Figure 2 shows DRIFTS spectra of S82 samples submitted to extreme pH conditions, compared with an F127-templated silica after template extraction. Inorganic framework Si−O−Si bands corresponding to transverse optical (TO) Si−O−Si modes can be observed in the 800 ($\nu_s$, or $TO_2$ mode) and in the 950−1300 cm$^{-1}$ zone ($\nu_{as}$, or $TO_3$ mode, accompanied by a longitudinal optical mode, which appears as a shoulder at 1250 cm$^{-1}$) for all samples.[36] Stretching $\nu_{CH}$ bands (2900−3000 cm$^{-1}$) corresponding to methylene residues belonging to the aminopropyl groups are present in hybrid samples after template extraction; several bands appearing in the zone of 1300−1500 cm$^{-1}$ correspond to C−H bending. Amino and/or ammonium functions are visible in the hybrid film samples as broad bands in the 3000−3500 cm$^{-1}$ region ($\nu_{NH}$), which superimpose to the large O−H stretching bands of adsorbed water and surface hydroxide groups with extended H-bonding. Si−O−H bands are observed at 950 cm$^{-1}$. Figure 2B shows a detail of the bending zone located in the 1500−1700 cm$^{-1}$, which is indeed informative: bending O−H bands corresponding to adsorbed water are centered at 1650 cm$^{-1}$. While spectra of pure silica samples present only $\delta_{O-H}$ bands, hybrid samples also display absorption bands corresponding to nitrogen-containing species, $\delta_{N-H}$. When S82 samples are submitted to acidic conditions, the band located at 1560 cm$^{-1}$ corresponds to the asymmetric N−H$^+$ bending.[37] In alkaline conditions, the asymmetric N−H bending band is recorded at 1590 cm$^{-1}$. The band shift in different conditions is in good agreement with previously reported data[15,38] and permits us to state that acid−base reactions involving amino groups take place. However, no quantitative speciation information could be obtained from these bands, when systems were submitted to different pH conditions, due to partial overlapping of these bands with the intense OH bending, as well as lack of precise standards. Similar features are observed in T82 and Z82 spectra, except that the intense Si−O−Si bands are replaced by Si−O−M bands at slightly lower frequencies,[39] indicating a good dispersion of the organosilane in the mesoporous matrix.

**Analysis of the Surface Chemistry.** The chemical speciation of the N-containing functional surface groups was determined by XPS. The penetration depth of these measurements was ∼9 nm (electron attenuation length ∼3 nm), and therefore XPS probes the film surface, pore openings, and film walls up to a thickness of ∼9 nm. Thus, XPS observes not only the N-containing functional groups attached to the topmost layer but also functional groups inserted in the top layers of the solid matrix.

Figure 3 shows representative N 1s XPS spectra for aminopropyl functionalized hybrid films containing Si, Ti, and Zr in extreme pH conditions. A complete figure for systems at all pH values is shown in the Supporting Information. In all cases, the N 1s XPS signal contains two components at ∼402 and ∼400 eV BE (peaks I and II, respectively). On the basis of their BE position and behavior with pH, both peaks can be attributed to ammonium (Peak I, $-NH_3^+$ at 402 eV) and amino (Peak II, $-NH_2$ at 400 eV) species on the film walls, surface, and pore openings, in agreement with previous reported values.[22−25] This peak assignment is consistent with the observed decrease of the high BE component (the peak related to the ammonium group) at higher pH. The quantification of the changes in the fraction of protonated amino groups at extreme pH values shows that complete interconversion between the two functions does not take place under our experimental conditions. This is due to a fraction of the functional groups being located within the walls, which is characteristic of co-condensation routes.[2c] However, by assessing the difference between the amine integrated signal at extreme pH values,

(36) Innocenzi, P. *J. Non-Cryst. Solids* **2003**, *316*, 309.
(37) Socrates, G. *Infrared and Raman Characteristic Group Frequencies*, 3rd ed.; J. Wiley and Sons: Chichester, 2001.
(38) Wang, X.; Tseng, Y. H.; Chan, J. C. C.; Cheng, S. *J. Catal.* **2005**, *233*, 266.
(39) Angelomé, P. C. Ph.D. Thesis, University of Buenos Aires, 2008. See also Zhan, Z.; Zeng, H. C. *J. Non-Cryst. Solids* **1999**, *243*, 26.

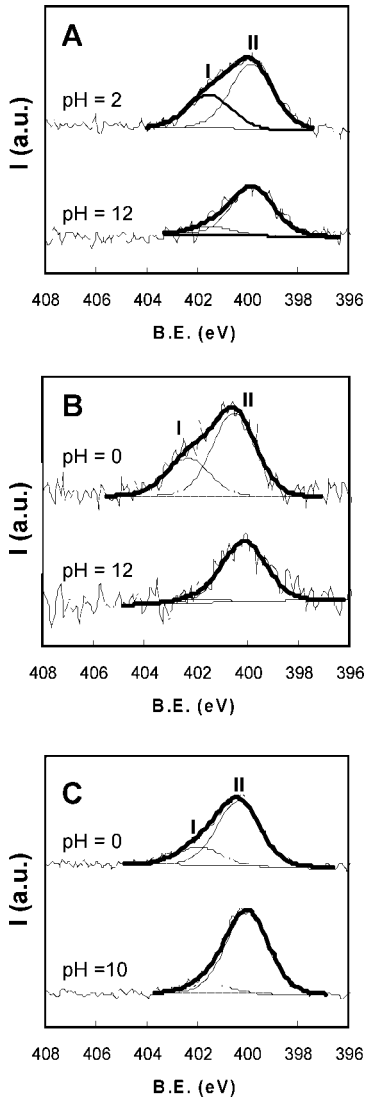


**Figure 3.** XPS N 1s spectra of (A) T82, (B) Z82, and (C) S82 hybrid films submitted to extreme pH values (indicated in each curve). Fitted peaks I and II resulting of signal deconvolution are shown in thin lines.

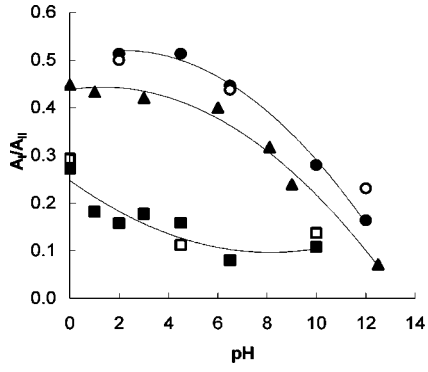


**Figure 4.** Evolution of the $R = A_I/A_{II}$ peak intensity ratio with pH. Squares, M = Si; triangles, M = Zr; circles, M = Ti. Closed symbols represent XPS analysis on deposited films; open symbols, analysis on scratched films. Curves in the figure are a guideline to the eye.

it can be determined that at least 20% of reactive surface functions are available on the surface, depending on the system.

Figure 4A shows the integrated peak area ratio $R = [-NH_3^+]/[-NH_2]$ as a function of pH for S82, T82, and Z82 films. Measurements performed on Si-supported thin films (full symbols) or on powder scratched films (i.e., presenting all possible orientations, open symbols) lie on the same curve, showing that the observed $R$ ratio represents a global behavior of the amino groups through the film and not only those located near the film surface. Two trends can be immediately distinguished: (a) $R$ decreases as the pH increases for all systems and (b) the pH dependence of $R$ changes with the chemical nature of M. These trends will be separately discussed below.

The first observation reflects the acidic character of the $-NH_3^+$ groups in M82 films (M = Si, Ti, Zr): as pH increases, the fraction of protonated amino groups (and therefore $R$) decreases, due to proton release from ammonium. Two differences can be observed with respect to soluble ammonium salts: (i) the speciation changes from ammonium to amine take place at relatively low pH values (ca. 1−2 for S82 and 6−8 for T82 and Z82), and the acidity of the ammonium group is higher compared to the value of $pK_a = 10.71$ for soluble propylammonium; (ii) the $R$ value changes in a broader pH range than the one corresponding to amine/ammonium in solution (details in the Supporting Information). Globally, the shape of the curves observed in this work resemble those of APTES-functionalized oxide surfaces[17,18,22,25] or amino-containing SAMs.[26] This behavior is well-known in polyelectrolyte or surface systems and can be attributed to the existence of a charged surface. At low pH values, the acidity of the ammonium groups is enhanced due to repulsion between their positive charges. The acid character of a surface is known to be pH-dependent; this has been rationalized by resorting to an effective constant at each pH value, $K_{eff}$.[40] XPS measuring conditions (high vacuum) can contribute an extra acidity enhancement, by eliminating water and displacing the acid−base equilibrium of the amino groups to the reagents; this was proposed for APTES-modified surfaces.[28] This is not a minor issue. Proton transfer from ammonium to surface $M-O^-$ groups might not be so strong in solution as it is observed in vacuum, due to the screening effect of the solvent and counterions. Recent work reports that the isoelectric point of amino-functionalized SBA-15 is in the range of 7−9 (compared to 2−3 for a pristine SBA-15), depending on the amino contents.[41] These values are attributed to the presence of amino functions, and their interaction with surface silanols. Although the $pH_{iep}$ might not necessarily reflect the acid−base processes taking place inside the pore systems, these values are an indicator of the possible range of speciation change in aqueous media. However, theoretical calculations on our own systems show that the proton transfer observed in our case takes place even in the presence of water mono- or bilayers (see below). In addition, the presented measurements are made on a variety of films under identical conditions, and the trends and general conclusions extracted are therefore comparable. Detailed DRIFTS experiments are in due course to compare the $K_{eff}$ values obtained in vacuo and in solution.

The second point to discuss is the different pH dependences of $R$ with the chemical nature of M. According to

(40) Holmes-Farley, S. R.; Reamey, R. H.; McCarthy, T. J.; Deutch, J.; Whitesides, G. M. *Langmuir* **1985**, *1*, 725.
(41) Rosenholm, J. M.; Lindén, M. *Chem. Mater.* **2007**, *19*, 5023.

**Scheme 1. Simplified Model for the Speciation and Interactions of the Surface Groups[a]**

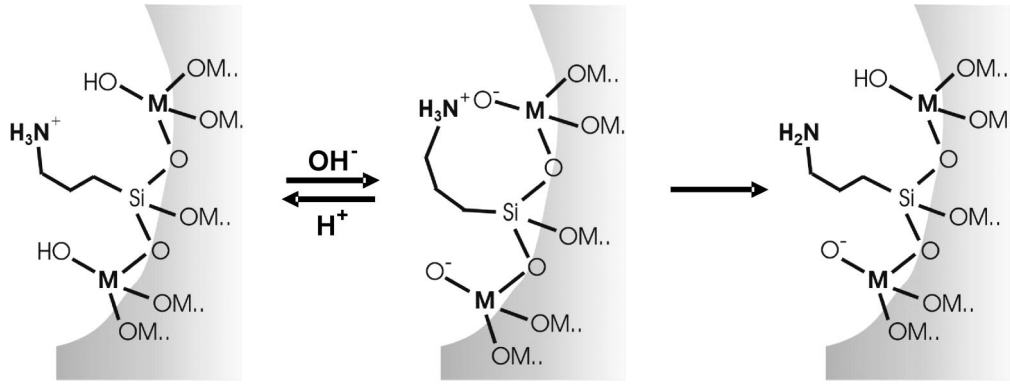


[a] For the sake of clarity, counterions are omitted.

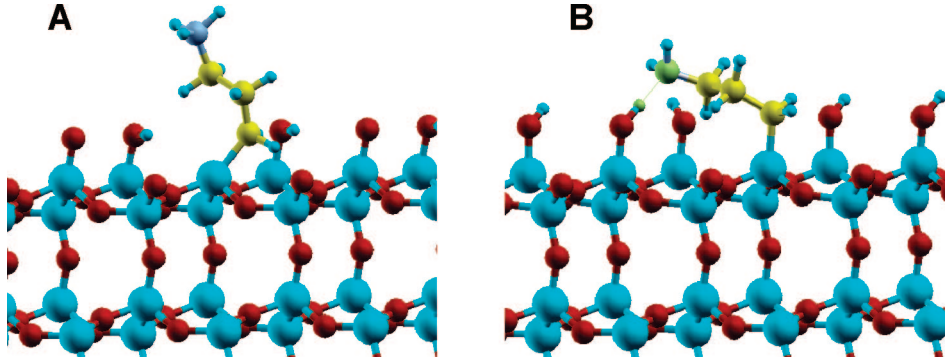


**Figure 5.** Initial (A) and relaxed (B) structures of an S82 surface, as obtained from DFT calculations in vacuum. The optimized geometry (B) exhibits a hydrogen bond between the M−OH and the $-NH_2$ functional groups.

Figure 4, there is a trend in the effective acidity of the ammonium group for these mesoporous matrices: S82 > Z82 ∼ T82. These observations seem to correlate with the surface acidity of the corresponding $MO_2$ oxides. Although surface p$K_a$ values present a large variability,[42] isoelectric point values ($pH_{iep}$) of the −M−OH surface groups can be an indicator to understand this trend. Silica surface has a reported $pH_{iep}$ value of 2, the $pH_{iep}$ values for titania and zirconia being 6−7 and 8, respectively.[43] Higher $pH_{iep}$ values imply less acidic −M−OH surface groups. The simplest model takes into account the "zwitterionic-like character" of the surface, which is a well-known behavior.[25,26] Previously reported titration measurements on aminopolysiloxane gels and powders in equilibrium with solution have established that ammonium is the major species, forming an ion pair with solution counterions at low pH, or interacting with $Si-O^-$ sites at higher pH values. Keeping this in mind, we can propose that deprotonation of M−OH sites at pH > $pH_{iep}$ leads to a strong interaction between $M-O^-$ groups and the less acidic propylammonium, which may actually "bend" onto the surface. Under the conditions studied, in the limit of very low water pressures, $-NH_3^+$ groups in the vicinity of $-M-O^-$ groups are unstable, leading to $-NH_2$ and −M−OH. Below $pH_{iep}$, ammonium and M−OH can coexist.

Our curves in Figure 4 indicate that the nature of the M−OH and R−$NH_2$ groups as well as their interplay determines the state of charge of the surface (Scheme 1). The acidity of the M−OH groups located near the amino groups should control the protonation of the $-NH_2$ function. The probability of finding a surface $-M-O^-$ group in the vicinity of an N-containing function should also be taken into account as a factor to control the $-NH_3^+/-NH_2$ ratio.

It is interesting to note that the method described here permits the surface charge and probably the conformation of the propylamino group to be modulated in a reproducible and tunable fashion by changing the element M which is co-condensed with the organosilane.

**Molecular Modeling of Surface Behavior.** To rationalize our findings, DFT calculations were performed on model systems of the functionalized titania and silica structures (periodic boundary conditions within a plane waves basis set scheme, Ti and Si oxide surfaces modeled using anatase and cristobalite slabs; see Experimental Methods). Geometry relaxations starting from an S82 or T82 surface in a zwitterionic configuration show that the $-NH_3^+$ function collapses on the surface to irreversibly transfer a proton to a neighboring $M-O^-$ group (see Figure 5). This result is in full agreement with the explanation given above to rationalize the trends observed in Figure 4 and the model proposed.

Under the experimental conditions corresponding to the XPS measurements, a small amount of water could presumably remain attached to the surface, affecting to some extent

(42) Contescu, C. I.; Schwartz, J. A. In *Surfaces of Nanoparticles and Nanoporous Materials*; Surfactant Science Series; Contescu, C. I., Schwartz, J. A., Eds.; Marcel Dekker: New York, 1999; Vol. 78, p 51.
(43) Kosmulski, M. *J. Colloid Interface Sci.* **2002**, *253*, 77.

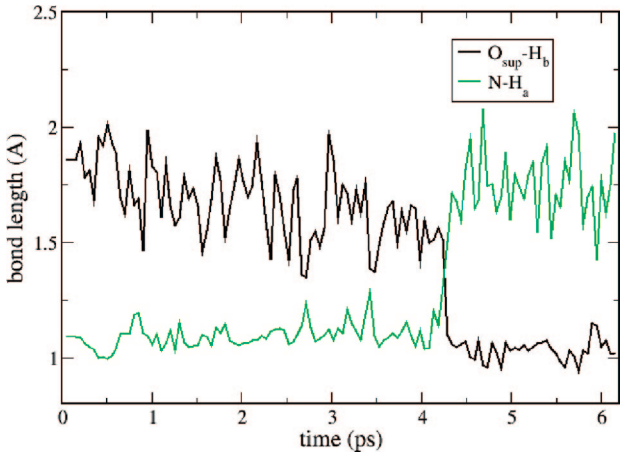


**Figure 6.** N−$H_a$ and $O_{sup}$−$H_b$ distances as a function of time according to a DFT molecular dynamics simulation on the functionalized silica surface, including two water monolayers. At zero time the system contains one $-NH_3^+$ group and one $-M-O^-$ function. $H_a$ is initially bonded to the ammonium group, while $H_b$ belongs to one of the water molecules acting as an intermediate. A concerted proton transfer resembling the Grotthus mechanism takes places at around 4.2 ps, to produce $-NH_2$ and −M−OH groups.

the $-NH_3^+/M-O^-$ equilibrium. To assess the feasibility of proton transfer in the presence of adsorbed solvent, molecular dynamics simulations including up to two water monolayers were conducted at ∼300 K on the silica surface. Two different runs starting from different (random) configurations showed that the transfer still proceeds through a concerted pathway resembling the well-known Grotthus mechanism for proton transfer. The $-NH_3^+$ moiety yields a proton to a proximate water molecule, which in turn transfers a second proton to the $-M-O^-$ surface group. This transfer is verified within a few picoseconds of simulation and leads to the formation of $-NH_2$ and M−OH, which now are not in direct contact. These calculations reinforce the proposed model, where the amino functions are prevalent, even in the presence of some water surface layers. This process is illustrated in Figure 6 for one of the simulations performed: the distances involving the transferred protons are plotted as a function of time. This mechanism suggests that the effect is not necessarily local; that is, the proton exchange may occur between groups which are not next to each other on the surface. We stress that in this system the ammonium and the hydroxyl groups are only partially solvated, representing some intermediate situation in between the vacuum and the bulk limits. It would be very interesting to determine how the $NH_3^+/M-O^-$ equilibrium changes with variable water content. Calculations to examine this question in detail are under way.

**Role of the Counterions.** The observed changes in the surface behavior should be also reflected in the contents and charge of the counterions in equilibrium. XPS measurements show low quantities of $ClO_4^-$ anions at low pH values (208 eV in Cl 1s spectra), for all examined samples. At higher pH values, $Na^+$ (1072 eV in Na 1s spectra) was detected (Figure 7a,b). These anions and cations counterbalance, at least partially, the positive and negative surface charges due to $-NH_3^+$ and $-M-O^-$ groups at low and high pH values, respectively. Figure 7c compares the changes in *R* and in $Na^+$ contents for T82 films along pH. A noticeable sodium

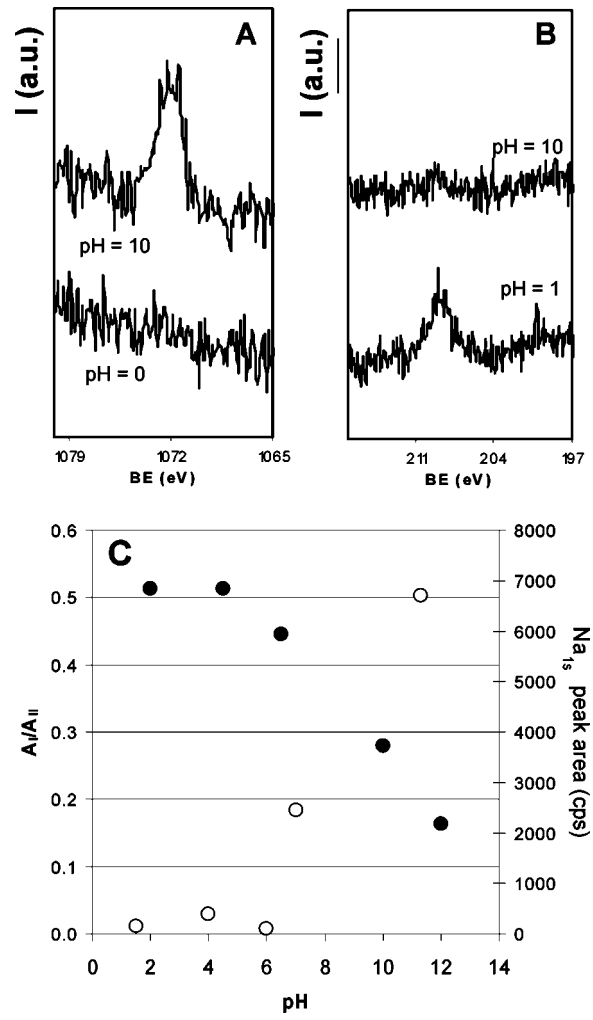


**Figure 7.** XPS spectra of the Na 1s (A) and Cl 1s (B) regions of S82 films, at extreme pH values (indicated in the figure) C. Evolution of $A_I/A_{II}$ (●) and XPS Na 1s peak area (○) with pH for T82 samples.

uptake can be observed for pH > 6. At these pH values, surface hydroxyls are acidic enough to release protons ($pH_{iep}$ = 6−7 for titania). Interestingly, ammonium speciation changes appreciably within the same pH interval. The same processes take place in silica- and zirconia-based systems: sodium uptake coincides with proton relaease in S82 and Z82 films (see Supporting Information). These findings reinforce the idea that the surface acidity of the oxide determines the speciation of the amino dangling species. For pH > $pH_{iep}$ of the matrix, the negatively charged $M-O^-$ sites attract sodium and ammonium cations. While ammonium cations can transfer protons to the $M-O^-$ sites, as previously discussed, sodium cations counterbalance the excess of negative charge. Similar trends of the behavior of *R* with solution pH and $Na^+$ uptake are observed in films with other compositions and in APTES-postfunctionalized silica.

**Role of a Second Function, Added by Postgrafting.** To test the whole behavior of the hybrid surface, we added a second function, PP, to Z82 and T82 samples at different pH values. PP is known to attach firmly to mesoporous zirconia and titania surfaces,[44] and therefore we would expect it to reduce the number of −M−OH surface groups vicinal

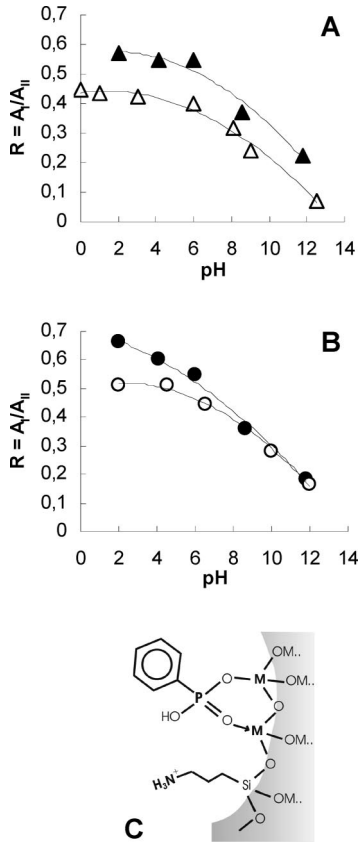


**Figure 8.** Evolution of the $R = A_I/A_{II}$ XPS peak intensity ratio with pH for Z82 (A) and T82 (B). Films were analyzed after template extraction (open symbols) or after exposing to PP solutions (closed symbols). Continuous curves are a guide to the eye. (C) Scheme of the ammonium conformation on the PP-modified pore surface.

to the N functions. Figure 8 shows that, at low pH, PP-modified mesoporous films present higher $R$ values, corresponding to a higher fraction of ammonium groups with respect to the nonmodified hybrid samples. This can be explained as follows: PP groups can efficiently complex Ti or Zr centers, acting as surface capping agents, as schematized in Figure 7c. The number of −M−OH surface groups vicinal to the N species thus decreases. This results in a lower number of interactions of the dangling ammonium with the M−OH/M−$O^-$ surface sites, leading to a higher $-NH_3^+$ fraction. At higher pH values a smaller "capping" effect is observed: XPS results (see Supporting Information) show lower P 2p/N 1s signal ratios, corresponding to lower PP contents, at higher pH. This is probably due to the lower PP sorption on a negatively charged surface. Therefore, the observed trends for the PP-modified films are similar to those observed in the absence of PP at pH > 8−9.

## Conclusions

This first detailed study of the global behavior of a system composed of an organic function and an inorganic wall in MHTFs demonstrates that even a simple organic group such as aminopropyl presents a relatively complex behavior on a pore surface. The speciation and conformation of the organic function depend on and are determined by the acid−base chemistry of a vicinal M−OH group. To understand the role of these aspects in the actual reactivity of the organic function, the interactions between the amino group and the surface must be taken into account. Indeed, the chemical availability of a dangling group or the hydrophilic−hydrophobic character of the pore surface can be modified by the acid−base behavior of the M−OH group. Thanks to the possibility of creating a uniform network of tailored vicinal groups with well-defined M centers, the behavior of the dangling organic function can be tuned by changing the nature of M. This tailoring of the function responsiveness to pH also implies conformation changes of the organic group at the surface, in contact with the solution, which can have an effect on the effective pore size but also on the hydrophilic/hydrophobic surface character. These points have a series of interesting implications in surface functionalization: attachment of biomolecules to surfaces, design of perm-selective or philicity-selective membranes,[3,17] or design of catalysts that show a well-defined organic reactive function near surface hydroxyl groups.[13] Experiments are in due course to adequately quantify the exposure of amino functions, their reactivity toward biomolecules, and their role in perm-selectivity.

**Acknowledgment.** This work has been funded by CONICET (PIP 5191) and ANPCyT (PICT Nos. 34518 and 33581), LNLS (D11A-SAXS1 Project Nos. 5867/06 and 6721/07; D10A-XRD2 Project Nos. 5872/06 and 5876/06) and Gabbos (GXNG 017). A.C. acknowledges TENARIS and CONICET for a collaborative graduate scholarship. P.C.A. acknowledges a CNEA-CONICET joint graduate scholarship. V.M.S. thanks CONICET for a graduate scholarship. I. Torriani, T. Plivelic, and G. Kellermann (LNLS, Brazil) are gratefully acknowledged for their assistance in XRR and SAXS measurements, and N. De Vincenzo (CMA, FCEN, UBA) is gratefully acknowledged for the TEM images.

**Supporting Information Available:** Detailed XPS spectra of M82 systems, evolution with pH of XPS spectra, XPS signal ratio, and comment on the effective acidity of the ammonium group (PDF). This material is available free of charge via the Internet at http://pubs.acs.org.

CM800597K

(44) (a) Angelomé, P. C.; Bilmes, S. A.; Calvo, M. E.; Crepaldi, E. L.; Grosso, D.; Sanchez, C.; Soler-Illia, G. J. A. A. *New J. Chem.* **2005**, *29*, 59. (b) Angelomé, P. C.; Soler-Illia, G. J. A. A. *Chem. Mater.* **2005**, *17*, 322.